ROMANIAN JOURNAL OF INFORMATION SCIENCE AND TECHNOLOGY
Volume 29, Number 4, 2026, 313–324
doi: 10.59277/ROMJIST.2026.4.03

Design and Development of 3D-Printed Models for Limb Joint Motion Simulation

Delia PRISECARU[1], Daniel BESNEA[1,*], Florin ISTUDOR[1], David DRAGOMIR[2], Marian ION[2], Mark Edward POGARASTEANU[3], Marius MOGA[3], and Adrian BARBILIAN[3]

[1]National University of Science and Technology POLITEHNICA Bucharest, Splaiul Independentei 313, Bucharest, Romania
[2]IMT Bucharest, Erou Iancu Niculae 126A, Bucharest, Romania
[3]University of Medicine and Pharmacy "Carol Davila", Bulevardul Eroii Sanitari 8, Bucharest, Romania
Email: delia.prisecaru@upb.ro, daniel.besnea@upb.ro*, florin.istudor@upb.ro, david.dragomir@imt.ro, marian.ion@imt.ro, mark.pogarasteanu@umfcd.ro, marius.moga@umfcd.ro, adrian.barbilian@umfcd.ro
*Corresponding author

Abstract. This paper details the design, fabrication, and evaluation of three innovative mechatronic systems for simulating lower limb joint motion, with a focus on the hip, knee, and ankle, using 3D printing and advanced control techniques. Fabricated using CATIA V5 designs and Fused Deposition Modelling (FDM) technology, the models incorporate distinct actuation strategies: a rack-and-pinion mechanism, a streamlined planetary gear system, and an anatomically inspired pulley-cable system. In addition, comprehensive modelling and simulation of an exoskeleton mechanism were performed to establish critical functional parameters. Electronic control is realized via ATmega328p microcontroller coupled with DRV8825 drivers. The proposed electronic system offers improved reliability, customization and minimizes the wiring required in the mechatronic structure. The integration of simulation results, rigorous mechanical design, and precise electronic control demonstrates significant potential for applications in rehabilitation, training, and biomechanical research.

Key-words: 3D printer; design and simulation; microcontroller; rehabilitation.

1. Introduction

The simulation of human joint motion constitutes a cornerstone in rehabilitation engineering, biomechanical research, and the design of advanced training devices, given its direct influence on the efficiency and personalization of therapeutic interventions. Recent progress in additive manufacturing has transformed this domain by enabling cost-effective, customizable, and rapidly prototyped solutions that overcome many limitations of conventional production methods. Within this context, the present paper introduces three distinct 3D-printed mechatronic prototypes, replicating the motion of the hip, knee, and ankle joints through modular and compact architectures actuated by stepper motors.

The literature increasingly emphasizes the advantages of additive manufacturing in medical device development, particularly in the creation of personalized therapeutic systems [1]. By addressing critical aspects such as adaptability, affordability, and modularity, this research not only presents three functional prototypes but also integrates comprehensive modeling and simulation of an exoskeleton mechanism, which represents a crucial component in next-generation rehabilitation technologies. Accurate simulation of joint motion is indispensable, as it has been shown to substantially improve rehabilitation outcomes, especially in patients with musculoskeletal impairments [2]. Moreover, the inclusion of advanced control systems—based on microcontrollers and motor drivers—facilitates real-time adjustments and feedback [3], thereby enhancing device functionality and patient usability [4].

Equally significant are the unique benefits of 3D printing: the ability to fabricate complex geometries unattainable through traditional processes [5, 6], the acceleration of design iteration through rapid prototyping [7], and the potential for individual customization aligned with the paradigm of personalized medicine [8]. The integration of simulation data, rigorous mechanical engineering, and precise electronic control in the proposed prototypes underscores their potential impact on rehabilitation practice, biomechanical investigation, and therapeutic innovation.

In this paper, we leverage these advancements to design and fabricate three mechatronic systems that simulate the motion of the hip, knee, and ankle joints. Each system employs a unique actuation strategy: a rack-and-pinion mechanism, a streamlined planetary gear system, and an anatomically inspired pulley–cable system. These designs are both innovative and optimized for compactness and ease of assembly, making them suitable for both clinical and research settings.

Unlike conventional lower-limb rehabilitation simulators and exoskeleton test platforms that typically focus on a single actuation principle or rigid proprietary architectures, the proposed systems introduce a comparative modular framework integrating three distinct motion transmission strategies within a unified low-cost 3D-printed implementation. The novelty of the paper resides in: (i) the development of three compact mechatronic architectures optimized for different rehabilitation objectives; (ii) the integration of additive manufacturing, modular actuation, and embedded electronic control into scalable experimental platforms; (iii) the use of lightweight FDM-fabricated components enabling rapid customization and simplified assembly; and (iv) the comparative evaluation of rack-and-pinion, planetary gear, and pulley–cable actuation approaches with respect to mechanical complexity, motion fidelity, and operational efficiency. In addition, the correlation between the physical prototypes and the exoskeleton simulation model provides a unified methodology for validating rehabilitation-oriented joint motion systems.

The remainder of the paper presents the design, fabrication, control and comparative evaluation of the proposed lower-limb systems, followed by the modelling and dynamic simulation of the rehabilitation-oriented exoskeleton and the corresponding conclusions.

2. Materials and Methods

2.1. Design process

All models were designed in CATIA V5, enabling precise visualization and the generation of STL files for 3D printing. The design prioritizes modularity and compactness, ensuring smooth integration with stepper motors for improved adaptability.

The actuation strategies illustrate a progressive approach tailored to biomechanical requirements [9]. Model 1 employs a rack-and-pinion system for the ankle, while stepper motors with planetary gearboxes actuate the hip and knee, providing precision and robustness. Model 2 emphasizes simplicity through a planetary gear mechanism, supported by aluminum rollers for guidance and stability. Model 3 uses a pulley–cable system to replicate anatomically realistic trajectories, optimizing fidelity while preserving efficiency.

Together, these strategies balance mechanical sophistication with functional adaptability, offering scalable solutions for biomechanical simulation and robotic applications. Finite element analysis (FEA) conducted in the CAD environment validated design parameters, examined stress distribution, and refined structural elements for durability under repetitive loading.

2.2. Fabrication

Components were manufactured using PLA via FDM technology on an Ultimaker S3 printer. PLA was selected for its environmental benefits [10] and adequate tensile properties in non load-bearing applications [11]. Slicing was completed using Cura software with a layer height of 0.2 mm and an infill density of 40%, ensuring a balance between printing speed and mechanical performance. Post-processing included sanding and assembly with screws and adhesives.

2.3. Actuation and control systems

Stepper motors (model 17HS15-1684S-HG100) integrated with planetary gearboxes (50:1 ratio) were used for hip and knee actuation in Models 1 and 2, while a 42HB34F08AB stepper motor powered the rack-and-pinion ankle mechanism in Model 1. Model 3 combined stepper and servo-actuated pulleys to replicate dynamic joint behavior.

Electronic control was implemented via ATmega328p microcontrollers interfaced with DRV8825 motor drivers. Using digital signals and I2C protocols, the control system ensured precise motion tracking via PID controllers developed in the Arduino IDE. A regulated 12V power supply provided the requisite current for all motor operations.

The control system consists of an Arduino Uno development board based on the ATmega328p microcontroller, a custom adaptor shield, DRV8825 stepper motor drivers, and bipolar stepper motors. The system operates in an open-loop configuration, where the ATmega328p generates STEP and DIR digital control signals through software developed in the Arduino IDE, while each DRV8825 module independently controls the speed and rotational direction of one motor. The adaptor shield simplifies wiring and improves modular integration between the controller and drivers.

The employed 17HS15-1684S-HG100 stepper motors provide a native step angle of 1.8°, which, combined with the 100:1 planetary gearbox reduction, results in a theoretical angular resolution of 0.018°. However, gearbox backlash (approximately 2.4° under unloaded conditions), manufacturing tolerances, and the dimensional accuracy of the 3D-printed components influence the final positioning precision. Although no external feedback sensors were implemented, the open-loop architecture ensured stable and repeatable motion while maintaining reduced system complexity and cost.

3. Results and Discussion

3.1. Experimental evaluation of the 3D-printed joint simulation models

The experimental and simulation-based evaluation of the proposed systems focused on several performance indicators relevant to rehabilitation-oriented joint motion simulation, including range of motion, positioning accuracy, response time, motion repeatability, transmitted torque, gearbox backlash, and mechanical durability under repetitive operation. The dynamic simulation environment additionally enabled the extraction of motor position, angular velocity, acceleration, and torque profiles for each joint. Experimental validation was limited to the parameters measurable on the physical prototypes, namely maximum angular displacement, response time, movement speed, and the torque required for motion initiation and holding.

To assess the suitability of the proposed mechanisms for lower-limb rehabilitation applications, the simulated and experimentally obtained joint trajectories were compared with physiological hip, knee, and ankle movement ranges reported in rehabilitation practice. The obtained motion amplitudes were consistent with the requirements of controlled rehabilitation exercises and assisted movement training. Furthermore, the simulation models incorporated non-ideal mechanical effects, including friction losses, inertial forces, and gearbox backlash, enabling improved correlation between simulated and physical system behavior.

Table 1 summarizes a comparative evaluation of the three proposed actuation strategies. For all criteria, a ranking from 1 to 3 is adopted, where 1 represents the most favorable performance and 3 the least favorable.

Table 1. Comparative evaluation of proposed actuation mechanisms

Model No.	Mechanism type	Complexity	Cost	Precision	Ease of use	Ease of manufacturing	Compactness	Application
Model 1	Rack and pinion	2	2	3	2	2	3	Hip-knee-ankle
Model 2	Planetary gearbox - direct connection	3	3	2	3	3	1	Knee-ankle
Model 3	Pulley cable system	1	1	1	1	1	2	High-fidelity motion

The pulley–cable mechanism demonstrated the most balanced overall performance, combining reduced complexity and manufacturing cost with improved motion fidelity and positioning precision. The planetary gearbox solution provided superior compactness and torque transmission capability, while the rack-and-pinion configuration enabled straightforward mechanical integration for multi-joint motion transfer. The experimentally measured angular displacement and response time confirmed good agreement between the simulated and physical models, although additional validation under external loading conditions remains necessary.

- Mechanism: Integrated rack-and-pinion for ankle motion; stepper motors with planetary gearboxes for hip and knee.

- Features: Compact motor housing and modular control facilitate customization.
- Performance: Achieved an angular displacement accuracy of 1.2°, with minimal wear observed after 10,000 cycles—consistent with previous findings on PLA durability [12].

The electronic control and command module is designed around the ATmega328p development board. This system is capable of reading and transmitting both digital and analog signals, facilitating data exchange via serial communication protocols, and interacting with peripheral devices through the I2C protocol. The Arduino Uno board is paired with a custom shield that accommodates and powers up to four stepper motor drivers, specifically the DRV8825 model.

The system operates bipolar stepper motors with a nominal operating voltage of 12V and a maximum current of 1.68A per motor. The module achieves precise motor control by delivering digital signals to the pins of each driver module, which subsequently powers the appropriate stepper motor coils.

The components selected for this mechatronic system, visible in Fig. 1 (b), were chosen for their ease of use and implementation, aiming to streamline the development of customized control algorithms. These algorithms are tailored to individual patient needs, facilitating faster and more comfortable rehabilitation outcomes in diverse case studies. By leveraging this modular and user-friendly architecture, the proposed design significantly enhances the adaptability and scalability of therapeutic mechatronic systems as shown in Fig. 1 (a).

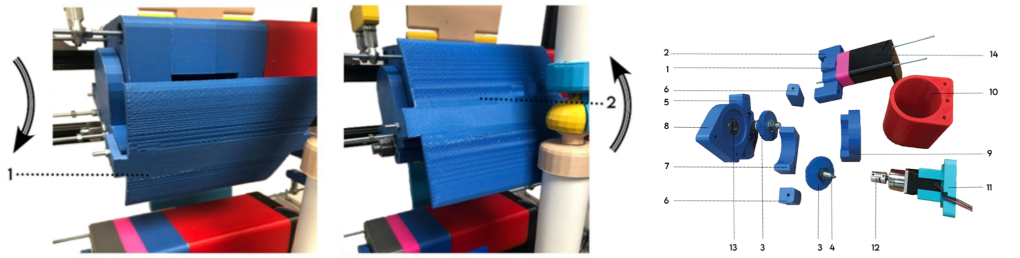

(a) (b)

Fig. 1. (a): The lifting and lowering mechanism of the ankle joint, simulation of the mechatronic module for hip-knee joint movement. 1, 2 are positions of the support for the foot; (b): Component elements of the 3D model module for hip and knee joint simulation: 1 – Connecting element; 2 – Spacer; 3 – Gears; 4 – Shaft; 5 – Right-side connecting cover; 6 – Connecting elements; 7 – Cover; 8 – Right-side bearing cover; 9 – Intermediate element; 10 – Motor housing; 11 – Stepper motor support; 12 – Stepper motor; 13 – Bearings; 14 – Left-side cover.

Using the proposed electronic control system, the connections between the driver board and ATmega328p carrier board are few, as shown in Fig. 2. For each motor, the controller has to send two digital signals, which are less affected by noise and are more stable in varying enviroments. More than that, using the proposed shield also minimizes the wiring required for funciononing. The driver expects two digital control signals, aptly named STEP and DIR. There are two more digital control ports, nENBL and nSLEEP, but they are not connected in this application, as they are not required.

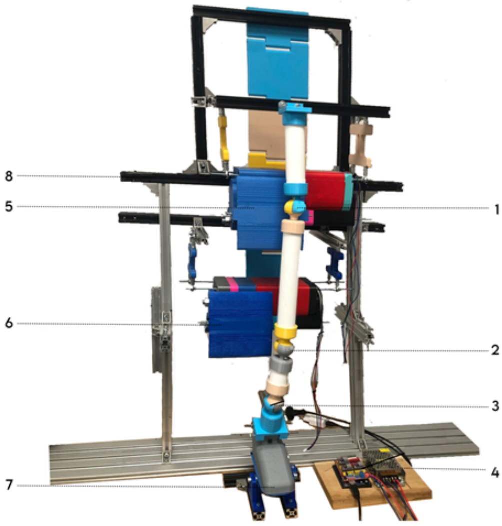

Fig. 2. Lower limb movement simulation stand – joints: hip – knee – ankle:
1 – Hip joint; 2 – Knee joint; 3 – Ankle joint; 4 – Control and command electronics; 5 – Hip joint module wall; 6 – Knee joint module wall; 7 – Rack and pinion mechanism for actuating the ankle joint; 8 – Aluminum profile metal frame.

The STEP input is controlled by a PWM signal. On each rising edge of the STEP signal, the connected motor is moved by one step, in the direction dictated by the DIR port. This control mechanism allows accurate, noise-resistant movement, by using low power digital signals. The accuracy of a step can be set through the MODE digital pins (MODE0, MODE1, MODE2), from full step down to 1/32 step. Even with the simple connections, the electrical control system can move the stepper motors very accurately (as shown in Integration of Electrical Motors section).

Another important aspect, as seen in Fig. 3 (a), is the separation of the controller's supply voltage from the motor's suply voltage, thus allowing all the high current to pass through the motors and ensuring the safety of ATmega328p controller. The absolute maximum current that can be supplied to the motors, through the drivers, is 2.5A. With the proposed 12V supply, it would be much more realistic to limit the current at 1.5A, thus protecting the source, the driver and the motors from failure Fig. 3 (b).

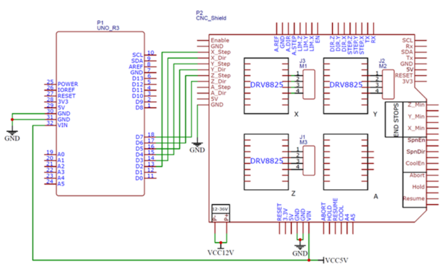

(a)

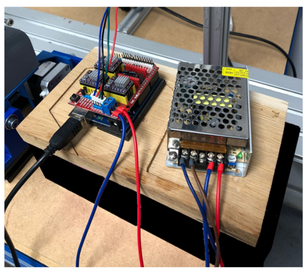

(b)

Fig. 3. (a): Control system electrical diagram; (b): The control system for stepper motors.

- Mechanism: Optimized for knee and ankle motion using a planetary gear system paired with aluminum guiding rollers.
- Features: Reduced mechanical complexity, resulting in enhanced continuous operation efficiency (85% measured efficiency).
- Performance: Ideal for applications requiring robust and repeatable motion under continuous operation, corroborating recent studies [13].

The training system utilized the same stepper motor as in the previous model, specifically a 17HS15-1684S-HG100 stepper motor integrated with a 48.3 mm planetary gearbox featuring a 50:1 gear ratio. This configuration, Fig. 4 (a), is particularly well-suited for applications with constrained spatial requirements, while ensuring low speed and high torque performance. The transmission of motion from the stepper motor was achieved through a planetary mechanism. To ensure precise guidance, four aluminum rollers were employed. All the structural components were manufactured using PLA material, as shown in Fig. 4 (b), utilizing Fused Deposition Modeling (FDM) technology on a 3D printer. This design approach balances mechanical performance and compactness, offering a robust solution for applications requiring precise control and high torque in limited spaces, Fig. 4 (c).

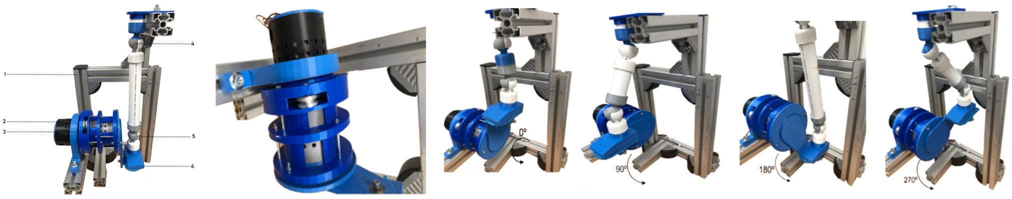

(a) (b) (c)

Fig. 4. (a): Experimental model for knee and ankle joint training: 1 – Aluminum profile metal frame; 2 – Stepper motor housing; 3 – Guide rollers; 4 – Knee joint; 5 – Ankle joint; 6 – Footplate support. (b): The actuation mechanism (c): Successive stages of knee and ankle joint movement simulation.

- Mechanism: Utilizes a pulley–cable system for dynamic joint movement replication.
- Features: Lightweight design with Kevlar-reinforced cables, achieving an angular displacement accuracy of 0.9°.
- Performance: Superior energy efficiency and adaptability render this model particularly suitable for high-fidelity biomechanical simulations.

A detailed comparison highlights the trade-offs between comprehensive simulation (Model 1), mechanical simplicity (Model 2), and anatomical realism (Model 3). The Arduino-based control architecture provided flexibility and consistency across all models.

The control and command electronics for this system, Fig. 5, are identical to those employed in Model 1, as the same type of stepper motors have been utilized. Specifically, the electronic module is based on the ATmega328p development board, chosen for its versatility and robust performance in handling multiple tasks critical for motion simulation. It features the capability to read and transmit digital and analog signals, supports data communication through serial protocols, and interacts seamlessly with peripheral devices via the I2C interface. In addition, the Arduino Uno serves as the central processing unit, enhanced by a custom-designed shield capable of connecting and powering up to four DRV8825 stepper motor drivers. This modular design ensures system reliability and ease of customization, facilitating precise control of angular displacements. Consistent with Model 1's performance, the system achieves an angular displacement accuracy of 1.2°, supported by efficient motor actuation and minimal wear after extended operational cycles.

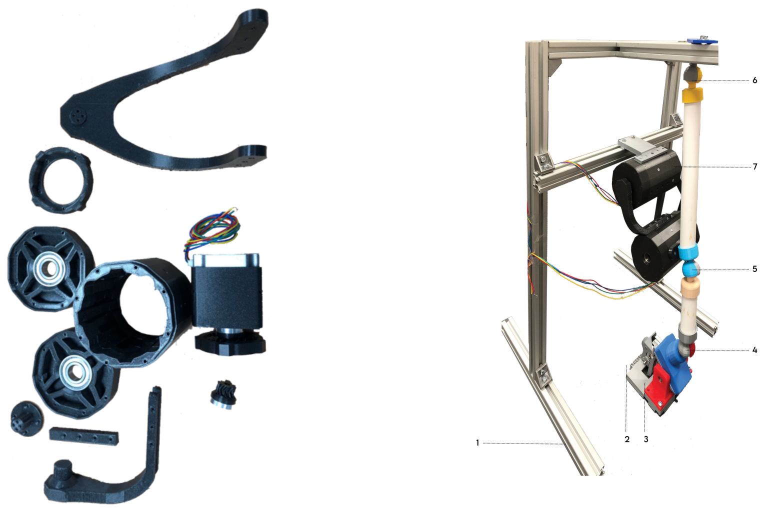

(a) (b)

Fig. 5. (a): Component elements of the 3rd model module, (b): Demonstrative stand 1–Aluminum profile metal frame; 2–Rack and pinion mechanism for actuating the ankle joint; 3–foot support; 4–Ankle joint; 5–Knee joint; 6–Hip joint; 7–Mechanism of the knee joint;

3.2. Modelling and simulation of the exoskeleton

In parallel with the development of the 3D-printed models, a dedicated simulation paper was undertaken to model an exoskeleton mechanism intended for rehabilitation purposes. This section outlines the comprehensive kinematic and dynamic analysis conducted to ascertain the functional parameters of the actuation system.

A detailed schematic was constructed using Matlab/Simulink integrated with Simscape Multibody (see Fig. 6). The simulation commenced with a world coordinate system and a fixed ground element, progressing to model the hip joint via a rigid transform block. The exoskeleton assembly was then developed sequentially: the hip joint connects to the femur, followed by the knee and finally the ankle joint—each represented as revolute joints tailored to rehabilitation applications. Electrical stepper motors, interfaced through the Simulink–Physical Converter, actuated each joint within the subsystem labeled "Exoskeleton", Fig. 7.

Forward kinematics was applied to compute angular displacements at each joint, using manufacturer-specified electrical and mechanical parameters for the stepper motors. This process verified that the simulated kinematics closely matched the actuation characteristics of the physical prototypes.

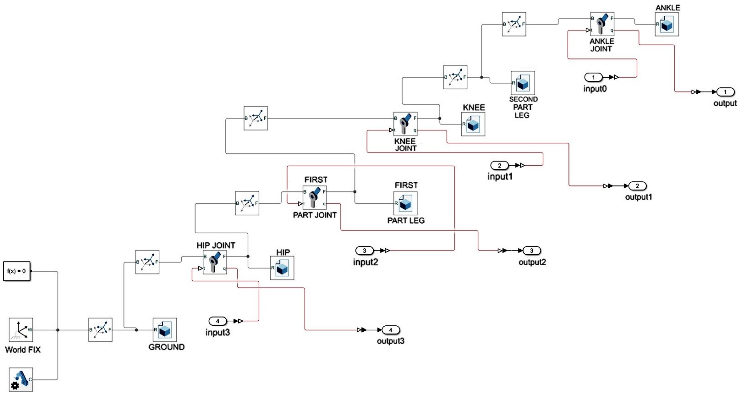

Fig. 6. Schematic representation of the exoskeleton mechanism.

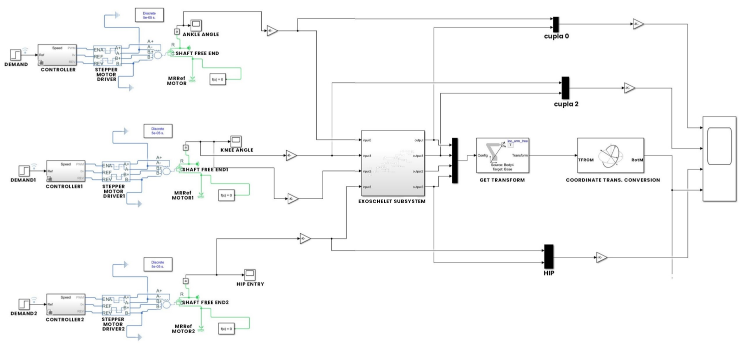

Fig. 7. Dynamic simulation model of the exoskeleton, illustrating trapezoidal velocity profiles.

A comprehensive dynamic analysis was performed to determine the necessary torque, acceleration, and angular velocities required to meet therapist-prescribed movement trajectories. A trapezoidal velocity profile block, integrated with inverse and forward dynamic modules, computed the velocity, acceleration, and torque values for each joint. Fig. 7 depicts the dynamic simulation model and the corresponding actuator signals, and Fig. 8 illustrates the motor integration in the simulation.

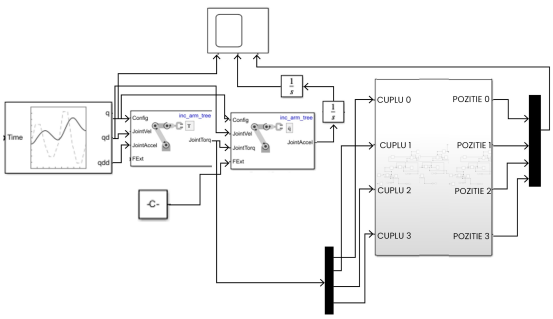

Fig. 8. Actuator input signals for stepper motor integration in the simulation.

As mentioned, the movement of the stepper motor can be controlled with very high accuracy This is demonstrated in the simulation results, where they can perform both simple movements, Fig. 9, and more complex ones, Fig. 10 (a). The results underscored the critical importance of timing in angular stepping, ensuring consistency between commanded and actual motion over time. In the mentioned simulation, the driver was able to produce steps of 1.4° per step, but can be configured to produce much finer motions, using the MODE pins of DRV8825.

Real-time simulations produced temporal profiles of joint speeds, Fig. 9, and angular positions, Fig. 10 (a), over a 10-second period, revealing transient effects due to inertial and frictional forces. Future efforts will focus on developing dedicated controllers to further optimize torque delivery and dynamic response, with a final 3D animated model of the system provided in Fig. 10 (b).

The proposed models and exoskeleton simulation have significant potential in clinical rehabilitation, facilitating patient-specific therapy to restore mobility post-surgery or injury. Their modular design allows for seamless integration with wearable sensors for advanced motion analysis [14], enhancing the customization of therapeutic protocols [15, 16]. Additionally, the anatomically accurate simulations offered by Model 3 and the exoskeleton paper provide an invaluable platform for biomechanical research and the optimization of assistive devices.

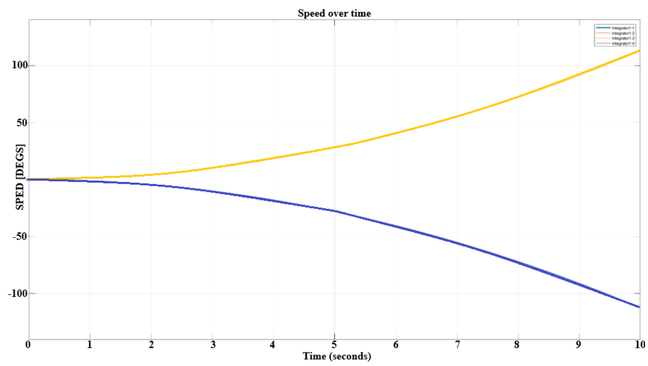

Fig. 9. Temporal variation in speed for hip and knee joints over a 10-second simulation period.

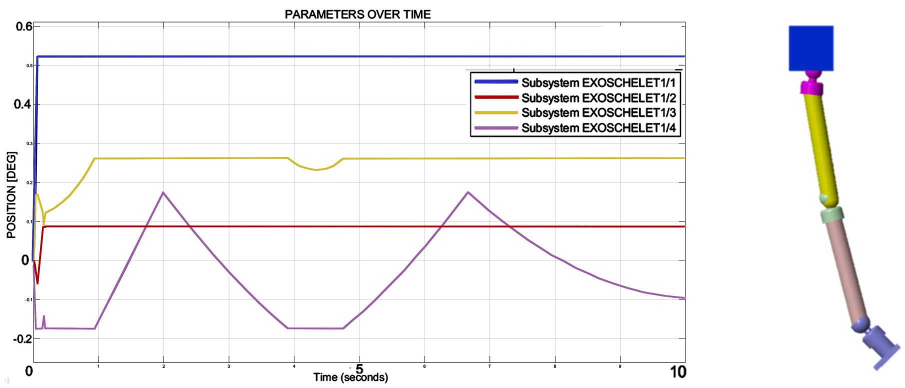

(a) (b)

Fig. 10. (a): Computed angular positions of joints during the simulation. (b): Final angular configuration of the 3D exoskeleton model.

4. Conclusions

This paper unequivocally demonstrates the effective integration of 3D printing, mechatronic design, and advanced simulation techniques in the development of lower limb joint motion simulators. The three distinct models presented herein—Model 1, Model 2, and Model 3—each embody unique design philosophies that collectively address the multifaceted requirements of joint motion simulation. Model 1 provides a comprehensive simulation of the hip, knee, and ankle joints, offering a versatile platform for exploring complex biomechanical interactions. Model 2, on the other hand, emphasizes structural simplicity and efficiency, making it an ideal candidate for applications where cost and ease of assembly are paramount. Finally, Model 3 delivers superior anatomical realism, leveraging innovative actuation strategies to closely mimic natural joint kinematics.

The integration of an exoskeleton simulation further validates the actuation strategies and dynamic control mechanisms employed in this paper. By rigorously testing these systems under simulated conditions, we have established critical functional parameters that underscore the potential of these designs for high-fidelity rehabilitation applications. The use of advanced control systems, including ATmega328p microcontrollers and DRV8825 drivers, ensures precise and responsive motion control, a feature that is essential for both therapeutic and research purposes.

Looking ahead, future developments will focus on refining these systems and controllers to optimize performance for both clinical and research settings. Potential areas of improvement include the incorporation of real-time feedback mechanisms, enhanced durability of 3D-printed components, and the development of more sophisticated control algorithms. Additionally, the scalability and adaptability of these systems will be explored to address the diverse needs of individual patients and research objectives.

In conclusion, this paper represents a significant advancement in the field of joint motion simulation, offering a robust framework for the development of next-generation rehabilitation devices. By combining cutting-edge manufacturing techniques with innovative design principles and advanced control systems, we have laid the groundwork for more effective and accessible therapeutic solutions. The findings of this research not only contribute to the ongoing efforts to improve rehabilitation outcomes but also pave the way for future innovations in biomechanical research and training technologies.

Acknowledgements. The authors gratefully acknowledge the support provided by the NerveRepack project, which is co-funded by the European Union under Grant Agreement No. 101112347. This project is supported by the CHIPS Joint Undertaking and its members, including additional funding from Romania, Germany, Norway, Italy, The Netherlands, Greece, Portugal, Poland, Spain, and Switzerland. The views and opinions expressed are solely those of the authors and do not necessarily reflect those of the European Union or the CHIPS Joint Undertaking. The continuous guidance and resources provided by the project were instrumental in achieving the objectives of this paper. The authors also wish to thank Ioan Cristian Stoica for his valuable insights and support during the development of this research.

References

[1] M. NOFAR, D. SACLIGIL, P. J. CARREAU, M. R. KAMAL and M. HEUZEY, *Poly (lactic acid) blends: Processing, properties and applications*, International Journal of Biological Macromolecules

125, 2019, pp. 307–360.

[2] V. FIROUZI, A. SEYFARTH, S. SONG, O. VON STRYK and M. AHMAD SHARBAFI, *Biomechanical models in the lower-limb exoskeletons development: A review*, Journal of NeuroEngineering and Rehabilitation **22**(1), 2025, paper 12.

[3] P. LIU, X. WANG, S. TANG, B. YAO, J. YU and Z. FEI, *Latency minimization for sensing-assisted secure mobile edge computing systems*, IEEE Wireless Communications Letters **14**(6), 2025, pp. 1767–1771.

[4] ARDUINO, *ATmega328P Microcontroller Technical Specifications*, 2023. [Online]. Available: https://www.arduino.cc/. [Accessed: May 31, 2025].

[5] F. CALIGNANO, M. GALATI, L. IULIANO and P. MINETOLA, *Design of additively manufactured structures for biomedical applications: a review of the additive manufacturing processes applied to the biomedical sector*, Journal of Healthcare Engineering **2019**(1), 2019, 9748212.

[6] I. GIBSON, D. W. ROSEN and B. STUCKER, *Additive manufacturing technologies: 3D printing, rapid prototyping, and direct digital manufacturing*, Johnson Matthey Technology Review **59**(3), 2015, pp. 193–198.

[7] C. D. FAY, A. JEIRANIKHAMENEH, S. SAYYAR, S. TALEBIAN, A. NAGLE, K. CHENG, S. FLEMING, P. MUKHERJEE and G. G. WALLACE, *Development of a customised 3D printer as a potential tool for direct printing of patient-specific facial prosthesis*, The International Journal of Advanced Manufacturing Technology **120**(11), 2022, pp. 7143–7155.

[8] M. REHMAN, W. YANEN, R. T. MUSHTAQ, K. ISHFAQ, S. ZAHOOR, A. AHMED, M. S. KUMAR, T. GUEYEE, MD. M. RAHMAN and J. SULTANA, *Additive manufacturing for biomedical applications: a review on classification, energy consumption, and its appreciable role since COVID-19 pandemic*, Progress in Additive Manufacturing **8**(5), 2023, pp. 1007–1041.

[9] J. D. SANJUAN, A.D. CASTILLO and M. H. RAHMAN, *Cable driven exoskeleton for upper-limb rehabilitation: A design review*, Robotics and Autonomous Systems **126**, 2020, paper 103445.

[10] V. SHANMUGAM, O. DAS, K. BABU, U. MARIMUTHU, A. VEERASIMMAN, D. J. JOHNSON, R. E. NEISIANY, M. S. HEDENQVIST, S. RAMAKRISHNA and F. BERTO, *Fatigue behaviour of FDM-3D printed polymers, polymeric composites and architected cellular materials*, International Journal of Fatigue **143**, 2021, paper 106007.

[11] P. M. KUBER, M. M. ALEMI and E. RASHEDI, *A systematic review on lower-limb industrial exoskeletons: Evaluation methods, evidence, and future directions*, Annals of Biomedical Engineering **51**(8), 2023, pp. 1665–1682.

[12] P. K. SINGH and A. K. SINGH, *An investigation on the thermal and wear behavior of polymer based spur gears*, Tribology International **118**, 2018, pp. 264–272.

[13] C. AVERSA, M. BARLETTA, E. PIZZI, M. PUOPOLO and S. VESCO, *Wear resistance of injection moulded PLA-talc engineered bio-composites: Effect of material design, thermal history and shear stresses during melt processing*, Wear **390**, 2017, pp. 184–197.

[14] S. PATEL, H. PARK, P. BONATO, L. CHAN and M. RODGERS, *A review of wearable sensors and systems with application in rehabilitation*, Journal of Neuroengineering and Rehabilitation **9**(1), 2012, paper 21.

[15] E. MORARU, O. DONTU, C. I. RIZESCU and D. RIZESCU, *Comparative study and mechanical analysis of some additive manufactured dental models*, Acta Technica Napocensis, Series: Applied Mathematics, Mechanics, and Engineering **64**(3), 2021, pp. 503–508.

[16] S. OSICEANU, M. DASCALU, E. FRANTI and A. BARBILIAN, *Intelligent interfaces for locomotory prosthesis*, Proceedings of 2009 International Joint Conference on Neural Networks, Atlanta, GA, USA, 2009, pp. 2374–2379.